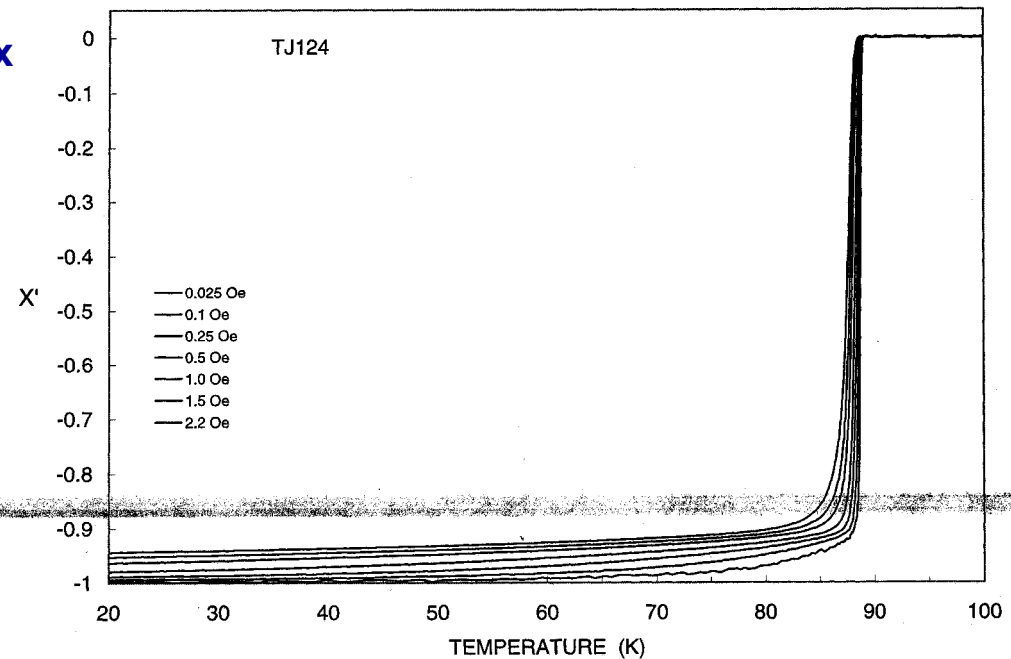
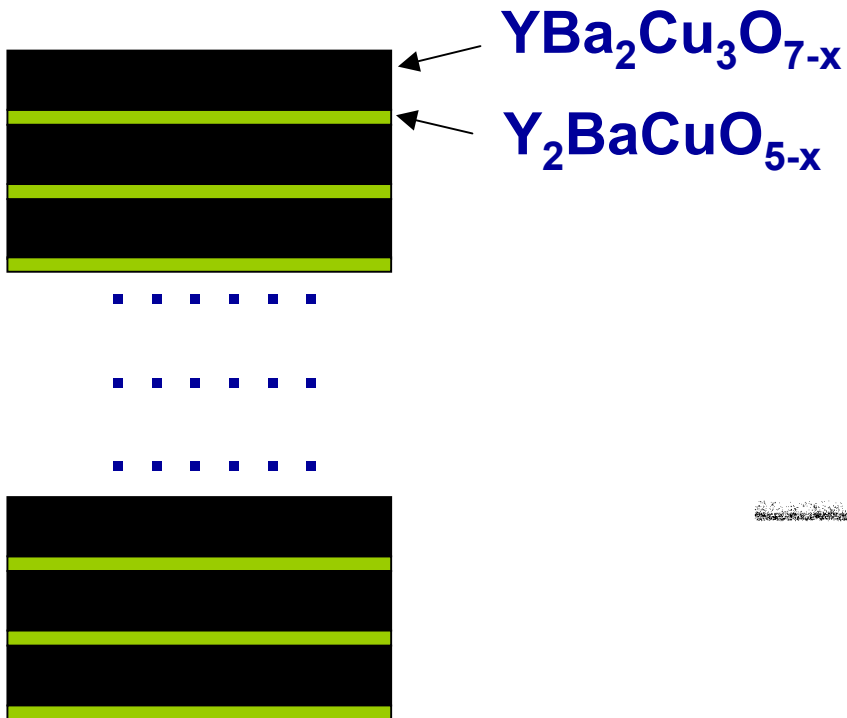




Multilayer Inclusions

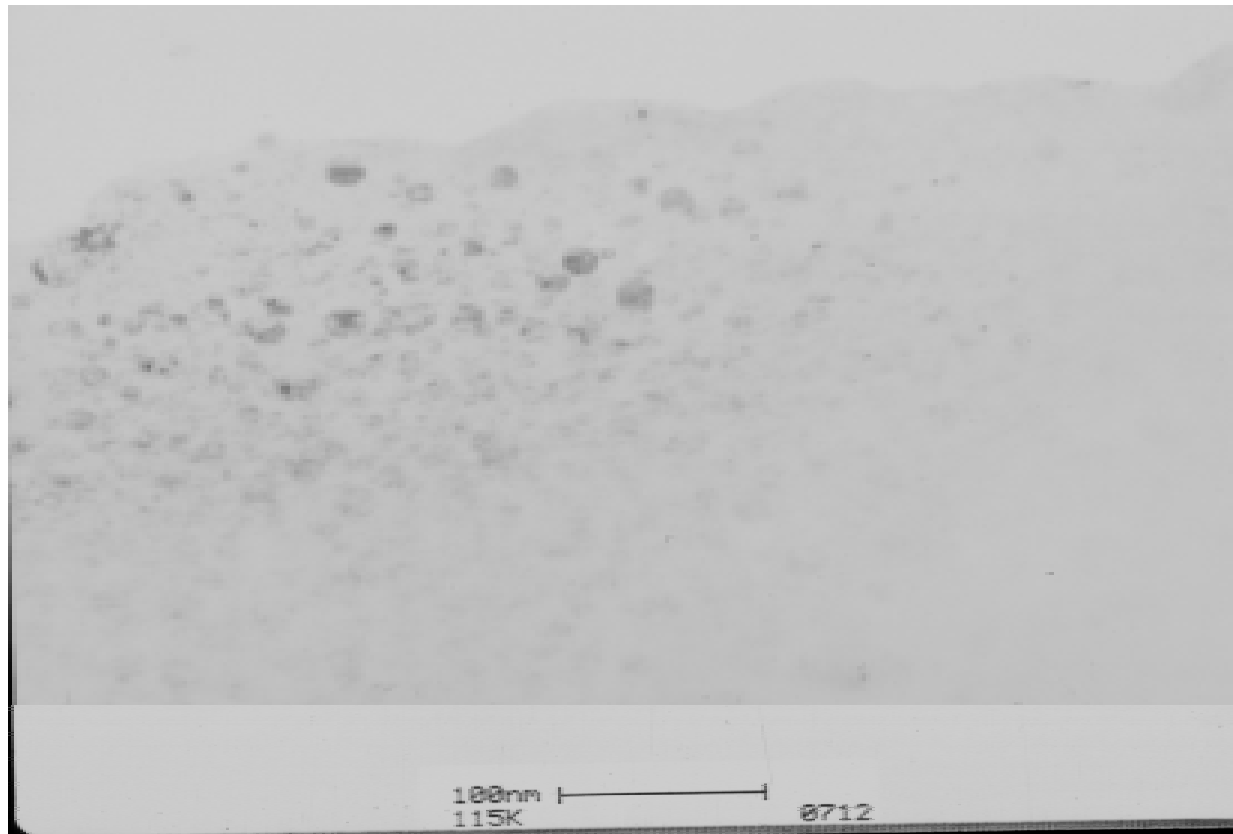


- Layers epitaxially grown by pulsed laser deposition
- 30 to 90 layers total -
 - Variable Y-123 thickness, Y123 = 4.6 - 15.0 nm, (Y211 = 1.0 nm constant)
 - Vary Y-211 thickness, Y211 = 1.2 - 3.8 nm, (Y123 = 15 nm constant)
- Sharp transition obtainable



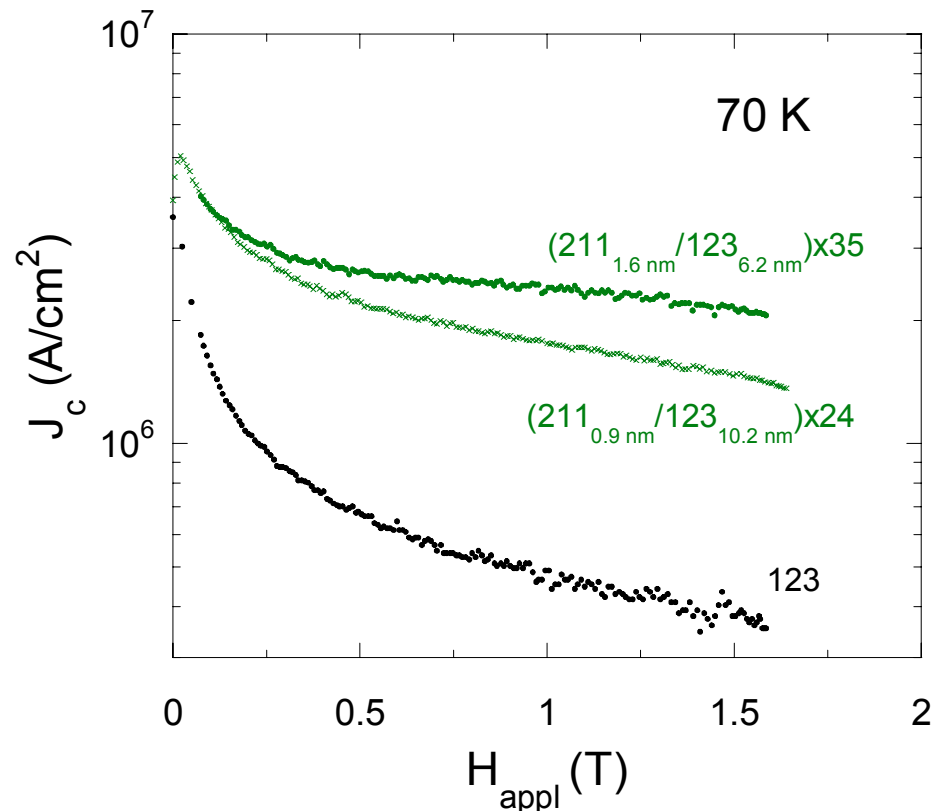


- TEM bright-field micrograph of the film looking through the planar view, showing the particle-like nature of all defects throughout the material.
- From planar views, the spherical nature of the particles is clearly seen with Moiré fringelike patterns. The Moiré patterns result when two phases are imaged that overlap with each other. The size of particles observed in Figure 1 was (10.8 ± 0.8) nm. Using this particle size, and assuming an aspect-ratio of ~ 4 , the particle density from mass balance was $\sim 7 \times 10^{11}$ cm⁻².



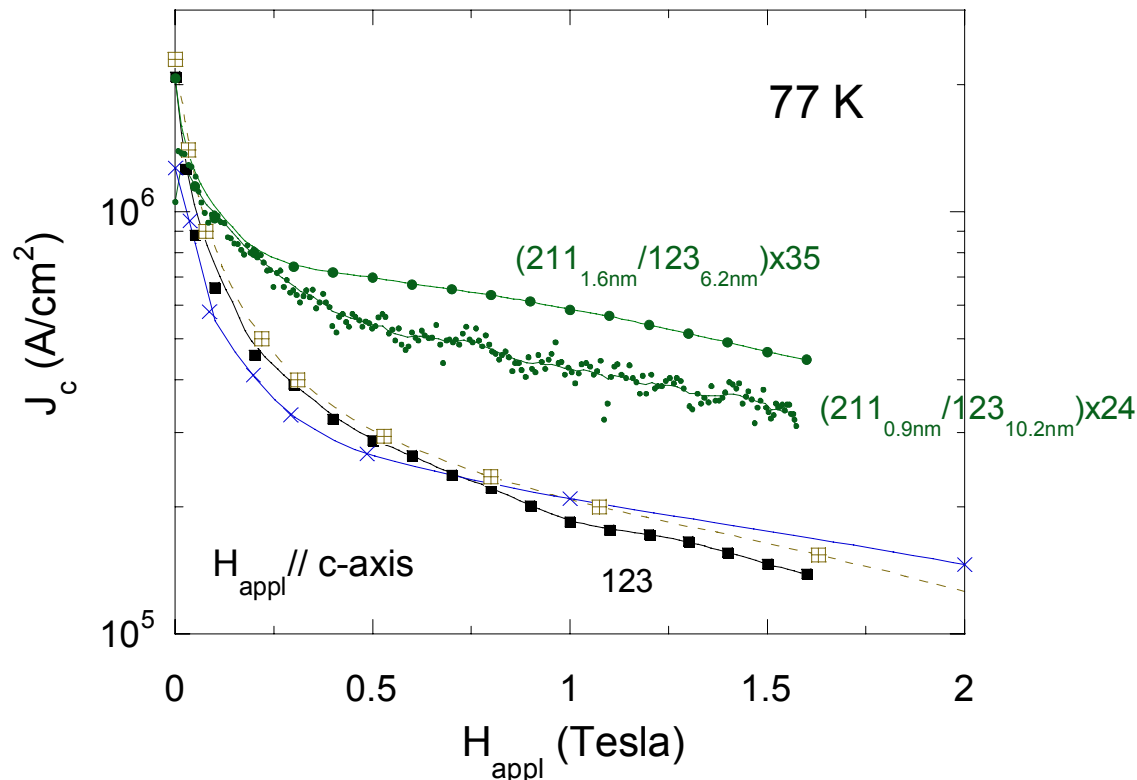


- J_c at 70 K as a function of applied magnetic field for a (2111.6nm/1236.5nm)x35 multilayer tape (●), compared to 123 films (■).
- The J_c s of (211~1.6nm/123~6.5nm)x35 multilayer tapes for zero applied field were in the order of 2-3 MA/cm², as determined by magnetic measurements in Figure 7 and also consistently measured by the 4-pt transport method on different samples. In Figure 7 at 70 K, a higher J_c was obtained for all applied fields, and the J_c increased > 500% for 1.6 T field.



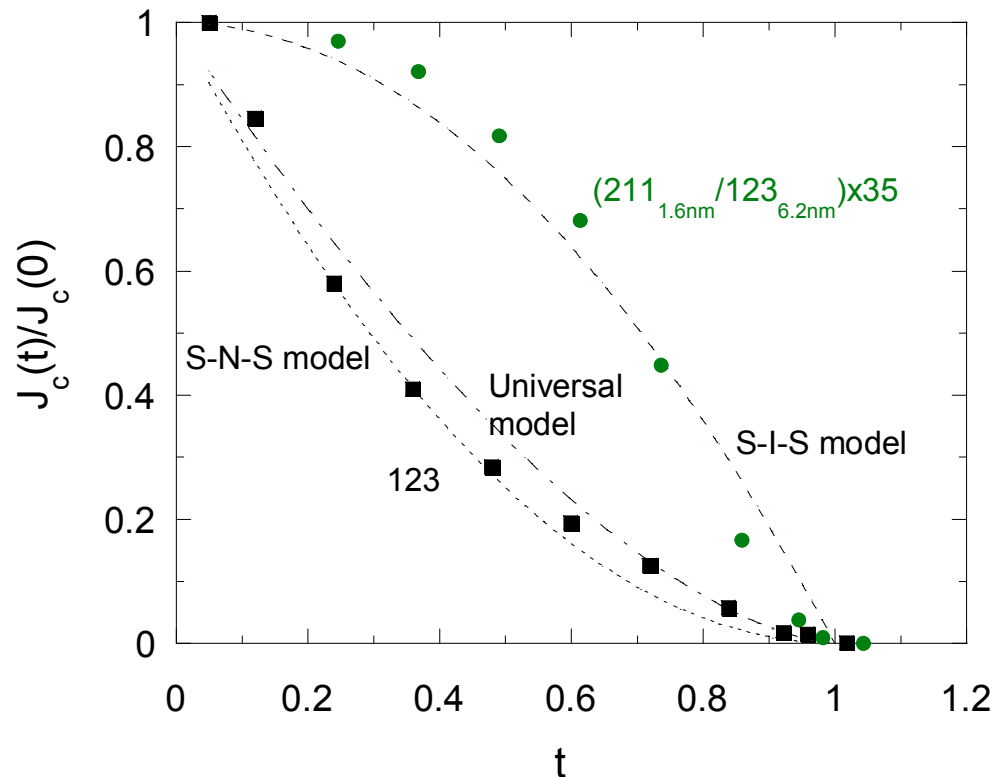


- J_c at 77 K as a function of applied magnetic field for 123 films on single crystal LaAlO₃ (●), compared to curves from the literature including YBCO on LaAlO₃ substrates at 75 K (□) [8], and YBCO on CeO₂/YSZ/Gd₂O₃/ RABITS (Ni,W,Fe) substrates (x) [9].
- An improvement of > 300% was achieved at 1.6 T, and the plots suggest that even greater improvement could be obtained at higher field strengths.





- The temperature dependence of $J_c/J_c(0)$ is plotted against a fit assuming different models of superconducting coupling []. Of the models tested, the J_c of the multilayers most closely matches the model of superconductor-insulator-superconductor (SIS) structures. Pinning by SIS structures for multilayers in Figure 9 also provides evidence that improvement of $J_c(H)$ in Figures 6-8 resulted from addition of 211 insulating defects, rather than the intrinsic defects such as strain induced dislocations.





- **Fig. 11. SEM micrograph of a (2111.2 nm/12310 nm)x100 multilayer film (left) ~ 0.9 micron thick compared to a 123 thick film (right) with similar thickness.**

